

https://dspace.org/

Effects of reaction pH on regular nanorods and hierarchically structured Ga2O3 and their isopropanol sensing capabilities

Nyepudzai Gatsi; Gugu H Mhlongo; Nosipho Moloto; Rudolph Erasmus; Odireleng Ntwaeaborwa

https://hdl.handle.net/10539/40454
SCOPUS

Downloaded from a DSpace repository. https://dspace.org/

MTLA 34 (2024) 102101

Contents lists available at ScienceDirect

Materialia

journal homepage: www.elsevier.com/locate/mtla

Full Length Article

Effects of reaction pH on regular nanorods and hierarchically structured β-Ga_2O_3 and their isopropanol sensing capabilities

Nyepudzai C. Gatsi [a], Gugu H. Mhlongo [b,*], Nosipho Moloto [c], Rudolph M. Erasmus [a,d], Odireleng M. Ntwaeaborwa [a,e,*]

[a] School of Physics, University of the Witwatersrand, 1 Jan Smuts Avenue, Braamfontein, South Africa, 2050
[b] DSI/CSIR Centre for Nanostructures and Advanced Materials, Council for Scientific and Industrial Research, Pretoria, 0001, South Africa
[c] School of Chemistry, University of the Witwatersrand, 1 Jan Smuts Avenue, Braamfontein, South Africa, 2050
[d] Microscopy and Microanalysis Unit, University of the Witwatersrand, Johannesburg, South Africa
[e] Sol Plaatje University, Department of Physical and Earth Sciences, Kimberley, South Africa, ZA8300

ARTICLE INFO

Keywords:
Gallium oxide
Isopropanol
Gas sensing
Nanorods
Nanobundles
Nanodandelions

ABSTRACT

Real-time detection of isopropanol is important for indoor air quality monitoring to improve human health. In this study, regular and hierarchical nanorod-based $\beta - Ga_2O_3$ morphological features were prepared using the microwave-assisted hydrothermal method following the variation of the reaction pH levels. A systematic study on their gas sensing performances was conducted to evaluate their potential as isopropanol gas sensing platforms. The sensor response and response times were directly controlled by morphology of $\beta - Ga_2O_3$. The randomly oriented $\beta - Ga_2O_3$ nanorods presented the highest response of 6.7 towards 90 ppm isopropanol while the $\beta - Ga_2O_3$ nanodandelions showed the fastest response/recovery times of 47/25 s. The observed variation in the gas sensing performances of the different $\beta - Ga_2O_3$ structures can be attributed to changes in morphological, textural, and compositional properties induced by the controlled reaction pH levels.

1. Introduction

Volatile organic compounds (VOCs) such as toluene, ethanol, benzene, acetone, and isopropanol are commonly found in commercial products including perfumes, cosmetics, and glues [1]. However, their substantial release to indoor environments may cause short-term and long-term adverse effects on human health. The short-term effects vary from irritation of the respiratory tract and eyes while the long-term effects may include cancer and renal failure [1,2]. In the case of isopropanol, continuous exposure and inhalation of 400 *ppm* may lead to mild and severe skin irritation and dizziness [3]. Therefore, real-time identification of isopropanol is vital for indoor environmental monitoring and control.

Spectroscopic techniques, such as chromatography, are currently utilized for the accurate detection of VOCs. However, these methods often require skilled personnel and expensive instruments, making chromatography challenging for real-time monitoring of the VOCs. Therefore, other portable, low-cost, and reliable methods for the detection of VOCs are being investigated. Different sensing materials have been studied for accurate detection of the VOCs. Among these materials, the chemiresistive semiconductor metal oxides (SMOs) gas sensors have gained a lot of attention due to their simple circuit design, easy and inexpensive fabrication process, long-term stability, and high sensitivity.

Among SMOs that have been previously explored for the detection of VOCs is gallium oxide (Ga_2O_3). Ga_2O_3 can crystallize in five polymorphic forms, namely $\alpha - Ga_2O_3$, $\beta - Ga_2O_3$, $\gamma - Ga_2O_3$, $\delta - Ga_2O_3$, and $\varepsilon(\kappa) - Ga_2O_3$. Among these polymorphs, the $\beta - Ga_2O_3$ is the most thermally stable hence mostly studied for gas sensing applications. In addition, $\beta - Ga_2O_3$, usually *n*-type, has a bandgap of $\sim 4.9\,eV$, high free electron concentration (10^{16} – 10^{20}), and electron mobility (200 $cm^2V^{-1}s^{-1}$), making it an appropriate candidate for application in gas sensing. Nanostructured 1*D* $\beta - Ga_2O_3$ materials have been extensively studied for the detection of various gases such as NH_3, O_2, CO at different operating temperatures [4]. However, challenges related to selectivity and high operating temperatures still hinder practical usage of $\beta - Ga_2O_3$ for gas sensing. Therefore, different morphological features from 1*D* to 3*D* exhibiting improved sensitivity are regarded as alternatives to overcome this challenge. For instance, one-dimensional

* Corresponding authors at: School of Physics, University of the Witwatersrand, 1 Jan Smuts Avenue, Braamfontein, South Africa, 2050.
E-mail addresses: gmhlongo@csir.co.za (G.H. Mhlongo), martin.ntwaeaborwa@wits.ac.za (O.M. Ntwaeaborwa).

https://doi.org/10.1016/j.mtla.2024.102101
Received 30 January 2024; Accepted 23 April 2024
Available online 23 April 2024
2589-1529/© 2024 Published by Elsevier B.V. on behalf of Acta Materialia Inc.

(1*D*) SMOs nanostructures such as nanowires, nanorods, nanobelts, have been found to exhibit excellent VOCs sensing capabilities owing to their high aspect ratio which offer fast electron transfer and more gas sensing activity sites. In addition, nanostructured 1*D* SMOs present unique physical and chemical properties. On the other hand, 3*D* hierarchical structures assembled from nanostructured 1*D* features have recently been generating interest as potential sensing material for the detection of VOCs. This is because they provide large surface area and particle-to-particle interaction which facilitate fast interfacial interaction and charge transport for enhanced sensor performances [5].

In the case of Ga_2O_3 materials, previous findings have revealed that their morphological behavior strongly depends on control of various parameters such reaction pH, among other things, during the synthesis process. For instance, Pilliadugula and Krishna [6] reported that when the *pH* condition is varied between alkaline and basic, the excess OH^- species are absorbed on the primary crystal facets, and this hinders the preferential growth thus favoring selective absorption of the OH^- ions. Under such conditions, the isotropic attachments and growth of *GaOOH* crystals with low-aspect ratio and hierarchical structures occur. Their findings revealed that *pH* variation from 7 to 14 resulted in the formation of nanorod-like, cocoon-like, and hierarchical structures. Besides, studies conducted on the utilization of undoped $\beta - Ga_2O_3$ as sensing materials for VOCs detection are still rare. Park et al. [7] produced $\beta - Ga_2O_3$-WO_3 heterostructures and observed remarkably improved sensor response and the response/recovery times towards 200 *ppm* ethanol at 200 °C compared to the ethanol sensing performances of undoped $\beta - Ga_2O_3$ nanostructures. The observed improved ethanol sensing performance was ascribed to synergistic effects of surface depletion and potential barrier-controlled carrier transport. Jang et al. [8] prepared $\beta - Ga_2O_3/SnO_2$ core-shell nanowires and demonstrated a high response of ~100 towards 1000 *ppm* of ethanol gas at a sensor operating temperature of 600 °C. Jin et al. [9] studied the effects of encapsulating $\beta - Ga_2O_3$ nanorods with *ZnO* on the NO_2 sensing capabilities of the material. The results demonstrated that the encapsulated nanorods presented a higher response towards 100 *ppm* that was presented by $\beta - Ga_2O_3$ nanorods [9]. Based on these previous reports on $\beta - Ga_2O_3$ as VOCs detection platform, the operating temperatures are still high, and sensitivity and selectivity require improvement.

This work was focused on the preparation of surface engineered 1*D* nanorods and 3*D* hierarchical $\beta - Ga_2O_3$ structures composed of nanorod features derived from a microwave-assisted hydrothermal method achieved through variation of the pH of reaction solution. The study was aimed at lowering the operating temperatures and improving sensitivity and selectivity of $\beta - Ga_2O_3$ structures towards isopropanol. The structural, morphological, and chemical properties of the synthesized $\beta - Ga_2O_3$ nanostructures were investigated and correlated with their gas sensing behavior recorded towards various gas analytes. The study developed $\beta - Ga_2O_3$-based gas sensors operated at low sensor operating temperature. A sensing mechanism involved in the observed gas sensing performance of $\beta - Ga_2O_3$ is proposed.

2. Experimental section

2.1. Preparation of $\beta - Ga_2O_3$ nanorod-based nanostructures

Gallium oxide hydroxide (*GaOOH*) powders were synthesized by microwave-assisted hydrothermal method prior to their conversion to $\beta - Ga_2O_3$ powders. To prepare pure *GaOOH* powders, three portions of 0.26 *g* of $Ga(NO_3)_3{\cdot}xH_2O$ (acquired from Sigma Aldrich, South Africa) were each dissolved in 10 *ml* of *DI* water, separately to obtain 0.1 M Ga^{3+} concentrated solutions. While vigorously stirring these solutions on a magnetic stirrer, all three solutions were heated to a constant temperature of 60 °C and the NH_4OH solution was added dropwise to the solutions to achieve different pH levels of 7, 11, and 14. The pH value of each solution was measured by a pH meter prior to aging of the solution for 1 h. The three solutions were transferred to the microwave vessels and microwaved for 1 h by using a Discover 2.0 microwave synthesizer set at 100 *W* and 150 °C. The resulting cloudy white precipitates were washed with distilled water and ethanol, then dried in an oven set at 60 °C to form *GaOOH* powders. The as prepared *GaOOH* powders were heat treated in air in a muffle furnace maintained at 750 °C, for 2 h, at a ramping rate of 5 °C/min to produce $\beta - Ga_2O_3$ powders. The powders were labelled pH7, pH11 and pH14 in line with the pH of each.

2.2. Sample characterization

The crystal structure and morphology of the powders were characterized by a Bruker D2 Phaser X-ray diffractometer with $\lambda_{CuK\alpha 1} = 0.15406$ *nm* radiation source and ZEIS-AURIGA field emission scanning electron microscope, respectively. The specific surface area and porosity of the powder samples were analyzed by a Micromeritics TriStar 300 analyzer. Chemical composition and defects were studied by X-ray photoelectron spectroscopy (XPS) using a PHI 5000 Versaprobe-Scanning ESCA Microprobe with monochromatic Al-Kα radiation ($h\nu = 1486.6$ eV).

2.3. Fabrication and testing of $\beta - Ga_2O_3$ nanorods-, nanobundles- and nanodandelions-based gas sensor films

To fabricate $\beta - Ga_2O_3$-based gas sensing films, 10 mg of each powder was ultrasonicated in 0.05 ml of ethanol to form a suspension which was drop-coated onto platinum electrodes interdigitated on an alumina substrate depicted in Fig. 1. All deposited films were annealed overnight at 300 °C for evaporation of ethanol and improve film-substrate adhesion. The gas sensing measurements were performed using a commercial KSGAS6S (KANOSISTEC, Italy) gas sensing station under both dry and humid atmospheric environments at different operating temperatures ranging from room temperature to 165 °C with a 2 *V* applied voltage across the sensors. Desired concentrations of the different gas analytes, in parts per million (*ppm*) were obtained as the ratios of synthetic air and compressed target gas using a mass flow controller (MFC). To achieve this, the flow rate of synthetic air was set at 500 standard cubic centimeter per minute and the MFC was programmed to control the flow of the test gas such that a desired concentration of the target gas reaches the test chamber. The target gases were commercially acquired in gas cylinders. The variations in electrical resistances across each sensor were acquired by a KEITHLEY 6487 picoammeter/voltage source meter in air (R_a) and target gas (R_g). The sensor response towards reducing and oxidizing gases was calculated from $\frac{R_a}{R_g}$ and $\frac{R_g}{R_a}$, respectively. The response time was measured as the duration taken to reach 90% of saturation resistance value and 10% above the base resistance upon injecting the target gas into the test chamber and stopping the target gas flow, respectively.

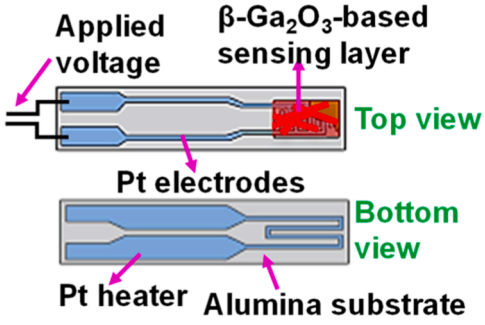

Fig. 1. Schematic representation of sensor setup.

3. Results and discussion

3.1. Crystal structure analysis of $\beta - Ga_2O_3$ powders

After the successful synthesis of $\beta - Ga_2O_3$ powders, their crystal structures were confirmed by XRD analysis, and the results are shown in Fig. 2. Diffraction patterns in Fig. 2(a) reveal that all the powder samples were readily indexed to the monoclinic phase of Ga_2O_3, i.e., $\beta - Ga_2O_3$ (Entry no. 96–200–4988). Moreover, Fig. 2(b) revealed that increasing the pH value resulted in higher diffraction intensities and a shift of the diffraction peaks to lower 2θ angles coupled with decreasing values of the full width at half maximum (FWHM) for the (111) crystallographic plane. The FWHM values were 0.53, 0.51 and 0.48 ° for the pH7, pH11 and pH14 powders, respectively. This observation suggests higher degree of crystallinity and larger crystallite sizes present on pH11 and pH14 powder samples. The average crystallite sizes for all samples were calculated from the most intense $\beta - Ga_2O_3$ diffraction peak corresponding to (111) using a Debye-Scherrer formula [10]. The crystallite sizes were found to be 16, 17, and 18 for pH7, pH11, and pH14 powder samples, respectively. The observed gradual increase in the crystallite sizes upon increasing the reaction pH value can be explained in terms of the increased rate of nucleation resulting from lowered degree of supersaturation of the $[Ga^{3+}]$ precursor solution [11]. At higher pH values, the surface of the adsorbent is negatively charged which increases the attraction of Ga^{3+} and crystal growth.

3.2. Morphology characterization of $\beta - Ga_2O_3$ nanostructures

The effects of varying reaction pH on the morphological behavior of $\beta - Ga_2O_3$ powders were further investigated by FESEM, and the results are presented in Fig. 3. Microstructures with different shapes, produced by agglomeration on the nanorods were observed from FESEM micrographs as shown in Fig. 3(a–c). A pH value of 7 induced the formation of randomly oriented regular nanorods with uneven edges resulting from random attachment of nanoplatelets-like structures. Increasing the reaction to pH levels of 11 and 14 resulted in attachment of regular nanorods forming 3*D* bundle-like and dandelion-like hierarchical structures, respectively. These results indicate the importance of the hydroxide ligand (OH^-) in the precipitation of the *GaOOH* precursor. According to Cüneyt *et al.* [12], when NH_4OH is added to the reaction, it decomposes to produce OH^- and NH_4^+ ions. Then, the OH^- ligand forms a complex with Ga^{3+} ions in the solution according to Eq. (1). Pilliadugula and Krishna [6] further stipulated that, generally, the OH^- ions preferentially adsorb along the *c*-crystallographic axis where there is low density of unsaturated bonds, leading to the formation of nanorod-like units in most hydrothermally synthesized *GaOOH* precursors. However, an increase in the pH value implies increased concentration of OH^- ions and a subsequent formation of a new complex $[Ga(OH)_3]^{3-}$ according to Eq. (2). This acts as a new growth precursor to the *GaOOH* seed obtained from Eq. (1). This results in the oriented attachments as observed from the pH11 and pH14 samples [11]. Yue *et al.* [13] also suggested that the addition of NH_4OH alters the surface energy of nanorods such that the nanorods self-assemble into an oriented format.

$$Ga^{3+} + 3OH^- \leftrightarrow Ga(OH)_3 \leftrightarrow GaOOH + H_2O \quad (1)$$

$$Ga(OH)_3 + OH^- \leftrightarrow \left[Ga(OH)_3\right]^{3-} + H_2O \quad (2)$$

Hereafter, the nanostructures prepared at pH values of 7, 11 and 14 are referred to as nanorods, nanobundles and nanodandelions, respectively.

3.3. Texture analysis of $\beta - Ga_2O_3$ nanorods, nanobundles and nanodandelions

Porous nanorod-based 3D structures are considered beneficial for gas sensing applications since they provide adequate space for gas diffusion into the sensing material, which results in fast response/recovery times [14]. For this reason, BET measurements were carried out and the nitrogen (N_2) adsorption-desorption isotherms of the $\beta - Ga_2O_3$ nanorods, nanobundles and nanodandelions are shown in Fig. 3(d). All $\beta - Ga_2O_3$ nanorod-based morphologies presented type IV(a) isotherms with H3 hysteresis loops with capillary condensation in the relative pressure range of $0.5 < P/P_0 < 1.0$ indicating that all samples were mesoporous [15]. The inset of Fig. 3(d) further revealed that the $\beta - Ga_2O_3$ nanorods, nanobundles and nanodandelions presented average Barrett-Joyner-Halenda (BJH) pore diameters of 22.1, 11.3, and 13.8 *nm*, respectively. In addition, specific surface areas of 15.8, 17.1, and 10.8 m^2/g were measured for these $\beta - Ga_2O_3$ nanorods, nanobundles and nanodandelions, respectively. These textural properties show that control of the pH induced variation in the porosity of hydrothermally synthesized $\beta - Ga_2O_3$ nanorod-based morphologies.

3.4. Chemical composition of $\beta - Ga_2O_3$ nanorods, nanobundles and nanodandelions

The material's capacity to adsorb charged oxygen species significantly influences its gas sensing performance [16]. However, this adsorption depends on the chemical state and composition of the sensing material. Therefore, to gain insights about the chemical composition of $\beta - Ga_2O_3$ nanorods, nanobundles and nanodandelions, XPS analysis

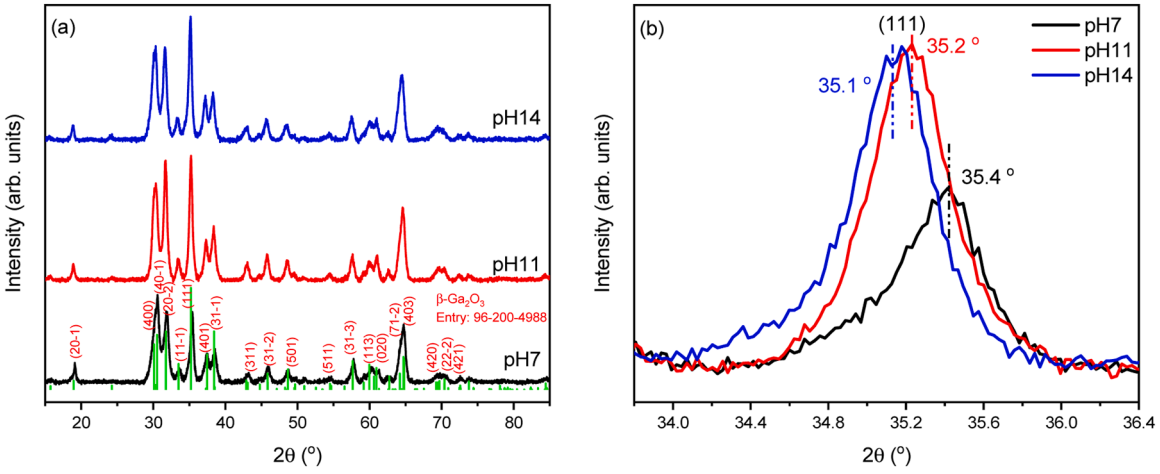

Fig. 2. XRD patterns of $\beta - Ga_2O_3$ powders prepared using a microwave-assisted hydrothermal method at different reaction pH levels.

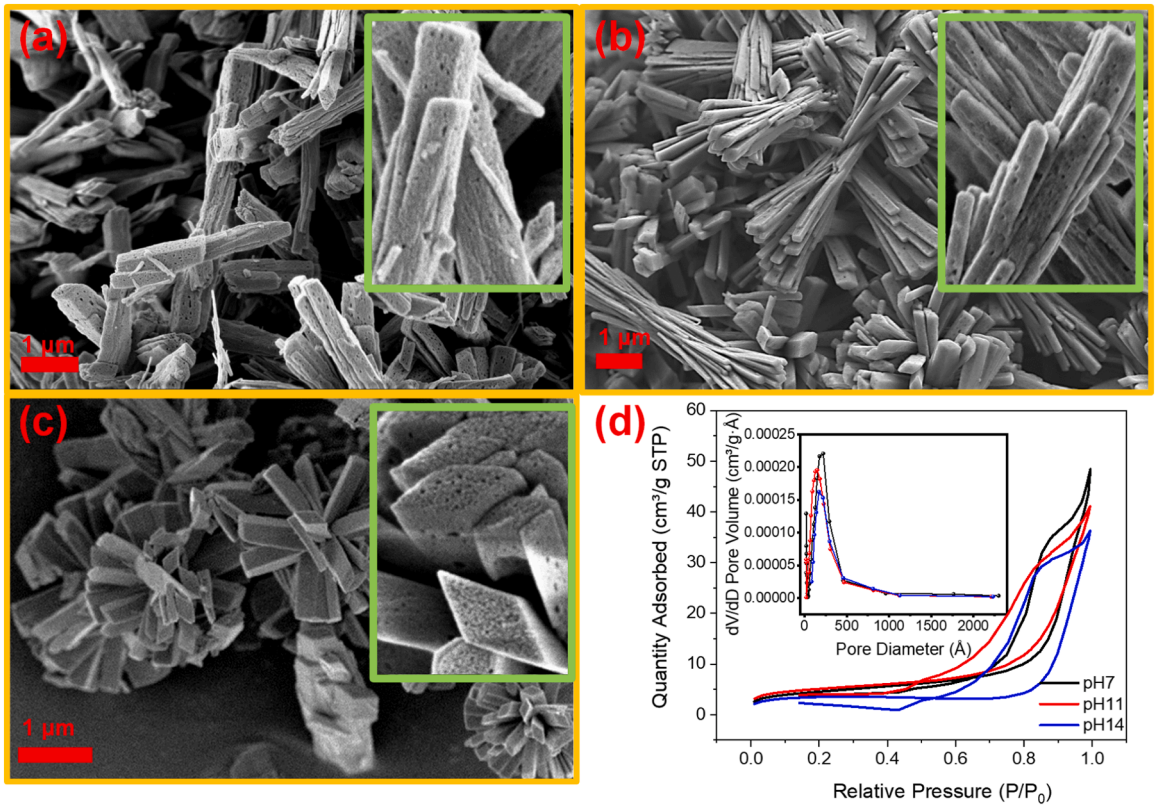

Fig. 3. FESEM images of $\beta - Ga_2O_3$ (a) nanorods, (b) nanobundles, and (c) nanodandelions prepared at the pH levels of 7, 11, and 14, respectively. (d) N_2 adsorption-desorption isotherms and pore size distribution of the nanorods, nanobundles and dandelions.

was conducted, and the results are presented in Fig. 4. All data was calibrated by the carbon peak at 284.8 *eV*. Firstly, Fig. 4(a) shows the high-resolution $Ga2p_{3/2}$ and $Ga2p_{1/2}$ spin-orbit doublet of the $Ga2p$ core-level separated by 26.9 *eV*; confirming the $Ga - O$ bonding in all samples [17]. Secondly, the quantity of oxygen species available at the surface of $\beta - Ga_2O_3$ nanorods, nanobundles and nanodandelions was determined by the analysis of the high-resolution $O\ 1s$ core-level XPS spectra presented in Fig. 4(b–d). The broad and asymmetric $O\ 1s$ components from all samples fitted with Gaussian peaks can be associated with chemisorbed oxygen (O_C), oxygen vacancies (O_V), and lattice oxygen (O_L) components [18], and their area contributions are indicated in Fig. 4(b–d). It can be noticed that the content of O_V increased in the $\beta - Ga_2O_3$ nanobundles and nanodandelions and this could probably be due to the removal of lattice oxygen [18]. In addition, the O_C content increased in the hierarchical structures, possibly due to favourable surface properties.

3.5. Gas sensor performances of $\beta - Ga_2O_3$ nanorods-, nanobundles- and nanodandelions-based gas sensors

The operating temperature of an SMO-based gas sensor significantly influences its gas sensing response by controlling the adsorption-desorption equilibrium of the target gas at the surface of the sensing oxide [19]. Hence, the effects of the sensor operating temperature on the gas sensing performance of $\beta - Ga_2O_3$-based sensors produced at 7, 11, and 14 pH levels were studied to determine their optimal operating temperatures. All sensors were exposed to 90 *ppm* isopropanol at operating temperatures from 25 to 165 °C and the results are shown in Fig. 5 (a). Response values obtained at 25, 40, and 60 °C are not included in the figure due to low signal to noise ratio. The recorded response curves revealed that initially all sensing signals improved with increasing operating temperature before reaching their optimum operating temperatures at 150 °C. This improvement could be attributed to the sufficient energy possessed by the isopropanol gas molecules participating in the reaction with the surface-adsorbed oxygen species. In addition, the generation of a high number of thermally excited electrons which subsequently facilitates the interaction between the target gas molecules and $\beta - Ga_2O_3$ nanorods-based sensing material may also be responsible for the improvement in the sensor response. However, a decrease in responses of all sensors was observed upon further increasing the operating temperature to 165 °C and this may be due to reduced number of active sites available for the adsorption of isopropanol gas molecules resulting from increased oxygen dissociation and adsorption on the active sites of $\beta - Ga_2O_3$ [20]. In addition, the rate of desorption of isopropanol gas molecules from the $\beta - Ga_2O_3$ surface is likely to be higher at high operating temperatures, hence the observed reduction in sensor responses.

To investigate the gas sensing behavior of these $\beta - Ga_2O_3$ based sensors exposed to various isopropanol concentrations, transient response curves were recorded with all sensors exposed to 5 – 90 *ppm* isopropanol at the optimum operating temperature of 150 °C. All sensor responses presented in Fig. 5(b) increased stepwise upon sensors' interaction with isopropanol and decreased back to baseline after the removal of isopropanol from the sensing chamber, confirming the typical *n*-type behavior of SMOs. Furthermore, the sensor responses displayed a continuous increase with increasing isopropanol concentration in the 5 – 90 *ppm*, and this can be attributed to the increased number of isopropanol gas molecules participating in the surface reaction. The $\beta - Ga_2O_3$ sensor produced at a pH level of 7 showed the highest response of 6.7 towards 90 *ppm* isopropanol compared to those produced at pH levels of 11 and 14 with responses of 0.5 and 1.4, respectively.

Besides high response, it is also important that for a sensor to exhibit a linear relationship between its response and concentration of the detected gas. To evaluate this relationship, the concentration-response data was plotted on a double-log scale for all $\beta - Ga_2O_3$ based sensors

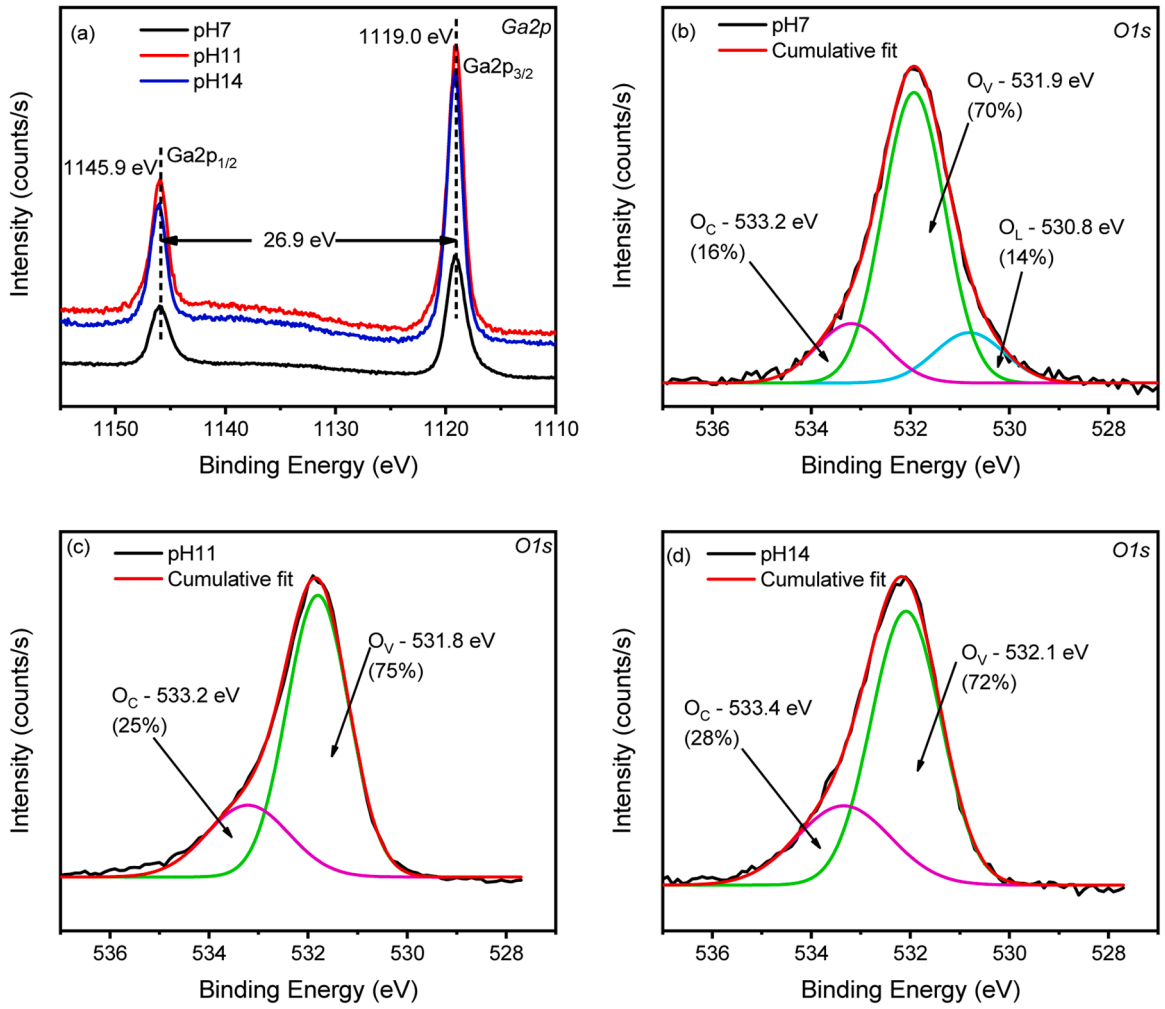

Fig. 4. High-resolution spectra of the (a) *Ga 2p* and (b-d) *O 1 s* core-levels for $\beta - Ga_2O_3$ nanorods, nanobundles and nanodandelions prepared under reaction pH levels of 7, 11 and 14, respectively.

and the results are presented in Fig. 5(c). All sensors showed good linear dependence ($R^2 \geq 0.96$) of the responses from 5 to 90 *ppm* of isopropanol. Furthermore, the sensitivities of 1.2, 1.7 and 1.3 ppm^{-1} for $\beta - Ga_2O_3$ sensors produced at pH levels of 7, 11, and 14, respectively, were extrapolated from the slopes of the linear curves fitted in Fig. 5(c) by using the linearized empirical power law of SMO-based gas sensors [21]. The limit of detection values of 0.6, 0.1 and 0.2 *ppm* were estimated as the lowest concentration of isopropanol that a sensor can detect with a 3:1 signal-to-noise ratio for the $\beta - Ga_2O_3$ sensors produced at pH level of 7, 11, and 14, respectively [22].

Another important characteristic of a gas sensor is its ability to selectively detect the gas of interest. To assess this capability, the responses of all $\beta - Ga_2O_3$ sensors towards 90 *ppm* of different VOC vapors and gases was measured. This test included other hydrocarbons (methanol and ethylene) which are likely to be present in indoor environments emanating from fruits or alcohols. Furthermore, toxic gases (i.e., carbon monoxide, hydrogen sulphide, sulphur dioxide, and nitrogen dioxide) which are likely to exist indoors and are harmful to human health were also considered in the comparison. The results presented in Fig. 5(d) registered higher responses to VOCs (i.e., isopropanol-C_3H_7OH and methanol-CH_3OH) than ethylene- C_2H_4, hydrogen sulphide- H_2S, carbon monoxide- CO, sulphur dioxide (SO_2) and nitrogen dioxide (NO_2). The high response towards VOCs may be attributed to the relatively low bond energy of isopropanol, methanol ($C-$C, 345 kJ/mol) compared to the bonds in ethylene ($C-H$, 415 kJ/mol), nitrogen dioxide ($N-O$, 469 kJ/mol), sulphur dioxide ($S-O$, 522 kJ/mol), carbon monoxide ($C-O$, 1072 kJ/mol), and hydrogen sulphide ($H-S$, 376 kJ/mol).

The response/recovery times of the $\beta - Ga_2O_3$ sensors were further measured, and the steady-state curves obtained are presented in Fig. 6 (a). It is demonstrated that the variation in morphology of $\beta - Ga_2O_3$ induced changes in the rate of reaction between the isopropanol gas molecules and the surface of the sensing material. In the present study, the dandelion-like structures ($\beta - Ga_2O_3$ sensor produced at a pH level of 14) presented the shortest response/recovery times and this may be attributed to the high number of contact points available promoting charge flow. In addition, the presence of more chemisorbed oxygen species facilitates the fast interaction and electron transfer between the target gas and the sensing material. The shorter recovery time recorded for the hierarchical structures ($\beta - Ga_2O_3$ sensor produced at pH levels of 11 and 14), compared to the regular nanorods ($\beta - Ga_2O_3$ sensor produced at a pH level of 7), may be caused by the fast desorption rate of isopropanol at these surfaces.

The practicality of a gas sensor also depends on the ability of the sensor to reproduce the sensing signal. The reproducibility of the $\beta - Ga_2O_3$ nanorods-based sensor was measured by exposing the sensor to consecutive cycles of 90 *ppm* isopropanol at an operating temperature of 150 °C and the transient curves obtained are shown in Fig. 6(b). All sensors exhibited good short-term stability with minor variations in the response values. Furthermore, the long-term stability of the sensor was also evaluated under the same conditions over a 30-day test period. The results presented in Fig. 6(c) revealed that all $\beta - Ga_2O_3$ sensors presented good long-term stability with the sensors presenting less than

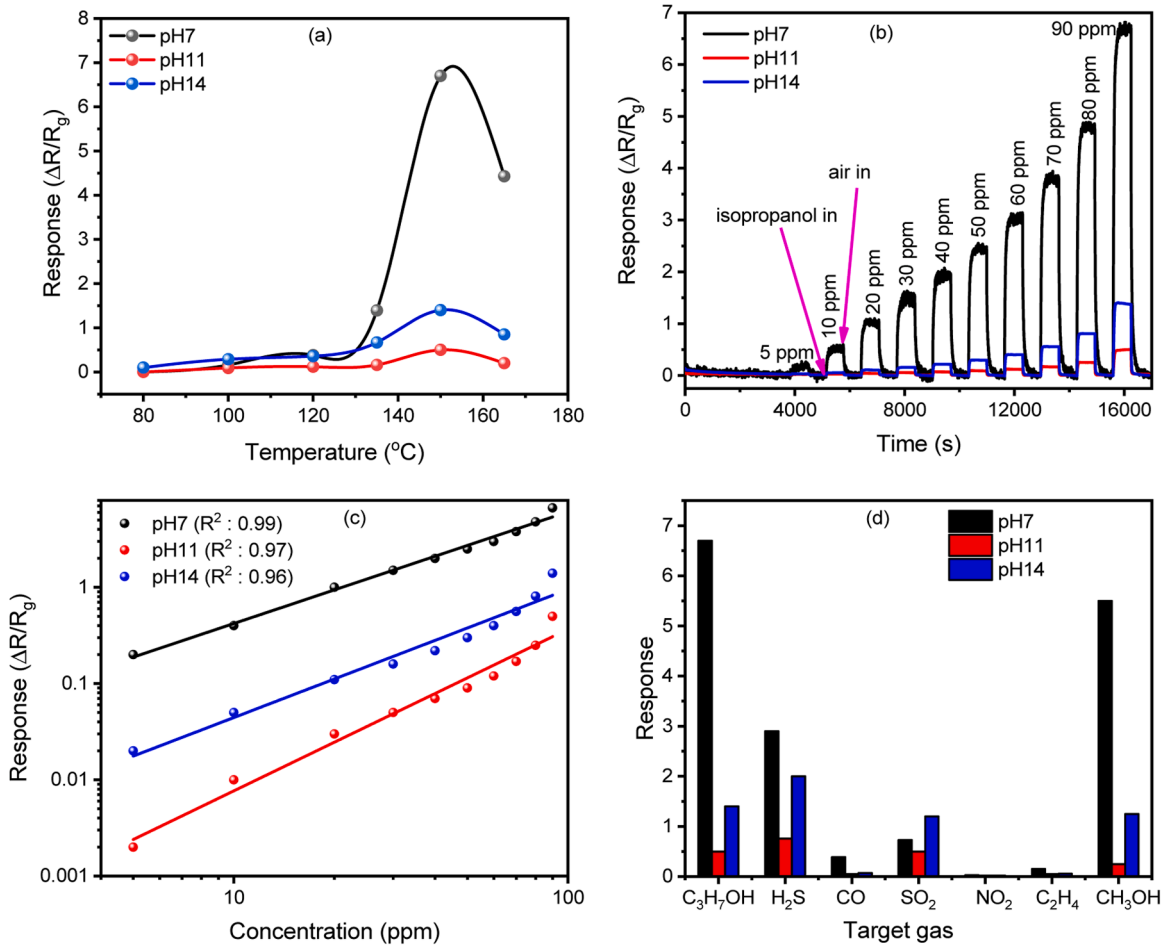

Fig. 5. Responses of $\beta - Ga_2O_3$ based sensors produced at pH levels of 7, 11, and 14, respectively, to 90 *ppm* isopropanol at different operating temperatures. (b) transient response curves and (c) corresponding double-log plots of $\beta - Ga_2O_3$ sensors produced at pH levels of 7, 11, and 14 exposed to 5 to 90 *ppm* isopropanol at 150 °C. (d) Sensor response towards 90 *ppm* of various gas analytes tested with sensors operating at 150 °C.

10% fluctuations from test day 20.

Environmental humidity affects the rate of gas adsorption and sensitivity of the sensing material, and this complicates the realization of sufficiently sensitive gas for real-world application. To study the impacts of humidity on the sensing performance of the prepared $\beta - Ga_2O_3$ sensing layers, the sensors were operated under 0%, 30% and 60% relative humidity (*RH*) conditions and their responses were compared. The data obtained from this comparison for the nanobunches and nanodandelions are not presented in Fig. 6(d) due to the low signal to noise ratio which made deduction of the response/recovery times difficult. The response and recovery times for pH7 sensor measured under the various RH conditions are indicated in Fig. 6(d). The curves reveal a decrease in sensor responses and prolongation of the response/recovery times upon introduction of water vapour molecules. The adsorption of water molecules on the sensing surface reduces the active surface area available for the adsorption of oxygen species and prolongs diffusion of gas molecules into the sensing material, resulting in the lower sensor responses and longer response/recovery times. Optimum response and response/recovery times from the randomly oriented nanorods were achieved under 0% *RH* sensing environments. Although there was a decrease in response, the sensor still retained 68 and 57% of its original response value when operated under 30%*RH* and 60%*RH* environments, respectively, which is a commendable result. This implies that the pH7 sensor can be used to effectively detect isopropanol in humid environments. The fast detection time displayed by this sensor under 0%*RH* conditions is essential for rapid detection of isopropanol.

Table 1 shows a comparison of VOCs gas sensors based on $\beta - Ga_2O_3$. As revealed in Table 1, the $\beta - Ga_2O_3$ nanorod-, nanobundles and nanodandelion-based sensors obtained in this study produced commendable gas sensing performances towards isopropanol. High response, fast response/recovery times were recorded at a lower operating temperature isopropanol.

3.6. Gas sensing mechanism of $\beta - Ga_2O_3$ sensors produced at pH levels of 7, 11, 14

The gas sensing performance of the SMO-based gas sensors depends on the change in sensor electrical resistance resulting from the sensing materials surface interaction with the target gas molecules [24]. Generally, when $\beta - Ga_2O_3$ nanorods (pH7), nanobundles (pH11) and nanodandelions (pH14) are exposed to air, oxygen molecules adsorb onto the surfaces of each nanostructure and get ionized to O_2^-, O^-, or O^{2-} species by trapping of electrons from the conduction band [19]. Consequently, the energy bands of these $\beta - Ga_2O_3$ nanostructures bend up causing formation of an electron depleted layer near surface of $\beta - Ga_2O_3$ nanostructures as presented Fig. 7(a, c, e). As a result, the electrical resistance of the $\beta - Ga_2O_3$ nanostructures (nanorods, nanobundles and nanodandelions) increases. The O^- type of oxygen species is adsorbed on the surface of these $\beta - Ga_2O_3$ since their optimal operating temperature was found to be 150 °C [24]. Upon exposure of the $\beta - Ga_2O_3$ nanostructures to a reducing gas (i.e., isopropanol), the gas gets oxidized by the chemisorbed O^- to form CO_2 and H_2O as shown by Eq. (1). As a result, electrons are released back to the conduction band of the $\beta - Ga_2O_3$ nanorods (pH7), nanobundles (pH11) and nanodandelions

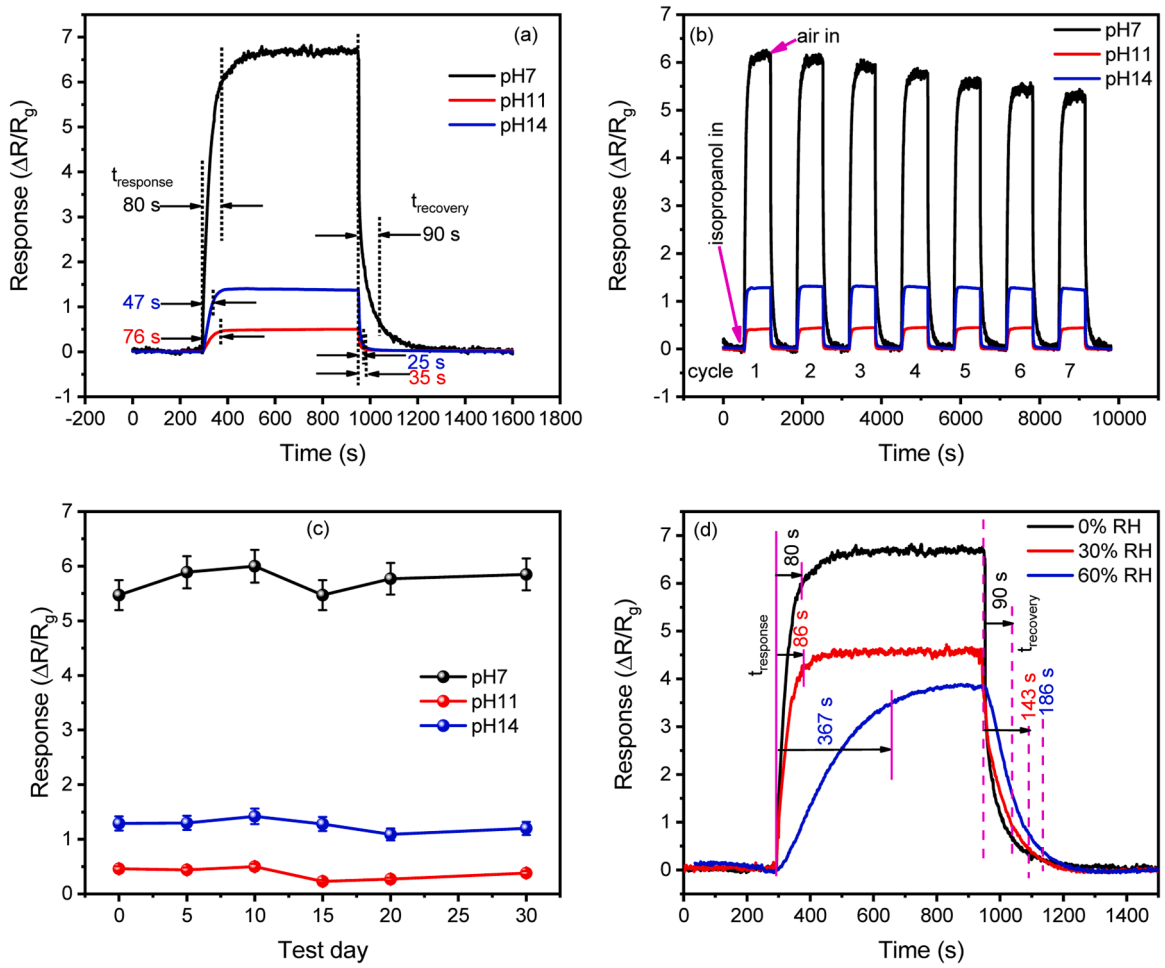

Fig. 6. (a) response times ($t_{response}$) and recovery times ($t_{recovery}$), (b) response reproducibility, and (c) response stability curves of the $\beta - Ga_2O_3$ sensors produced at pH levels of 7, 11, and 14 operated at 150 °C. (d) Responses and response/recovery times of the pH7 sensor under 0 % relative humidity (RH), 30 %RH and 60 %RH conditions. All sensors exposed to 90 *ppm* of isopropanol.

Table 1
Isopropanol detection capabilities of various Ga_2O_3-based gas sensors.

Sensing material	Gas	*T* (°C)	Conce. (*ppm*)	Response	t_{resp}/t_{reco} (*s*)	Ref.
Ga_2O_3/SnO_2 core-shell NWs	Ethanol	400	1000	$60\left(\frac{R_a}{R_g}\right)$	—/–	[8]
Ga_2O_3-core/WO_3 shell NWs	Ethanol	200	200	$\sim 540\left(\frac{R_a}{R_g}\times 100\%\right)$	~20/~130	[7]
Ga_2O_3 nanowires	Ethanol	200	200	$\sim 210\left(\frac{R_a}{R_g}\times 100\%\right)$	~20/~185	[7]
$CuO:Ga_2O_3$ films	Acetone	300	0.25	$\sim 1.1\left(\frac{R_g}{R_a}\right)$	394/563	[23]
$\beta - Ga_2O_3$ nanorods	Isopropanol	150	90	$6.7\left(\frac{R_a}{R_g}-1\right)$	80/90	This work
$\beta - Ga_2O_3$ nanobundles	Isopropanol	150	90	$0.5\left(\frac{R_a}{R_g}-1\right)$	76/35	This work
$\beta - Ga_2O_3$ nanodandelions	isopropanol	150	90	$1.4\left(\frac{R_a}{R_g}-1\right)$	47/25	This work

(pH14) and their electrical resistances are lowered as shown in Fig. 7(b, d, f).

$$C_3H_7OH_{(g)} + 9O^-_{(ads)} 3CO_{2\ (g)} + 4H_2O_{\ (g)} + 9e^- \quad (3)$$

The high response recorded form the $\beta - Ga_2O_3$ sensor produced at a level pH7 maybe attributed to the high porosity of the morphology compared to those produced at pH levels of 11 and 14 as observed from BET analysis. On the other hand, the high content of the chemisorbed oxygen observed from XPS results might also have contributed towards low sensor response of the nanobundles (pH11) and the nanodandelions (pH14) by reducing the active sites available for the adsorption of charged oxygen species and isopropanol gas molecules. In addition, although the limited accessibility to the individual nanorod surfaces in the nanobundles and nanodandelions by the isopropanol molecules may have contributed towards the observed low responses, the high contact networks in these hierarchical morphological features could be responsible for their high sensitivities and fast response kinetics (i.e., response/recovery times). The contact networks increase the number of

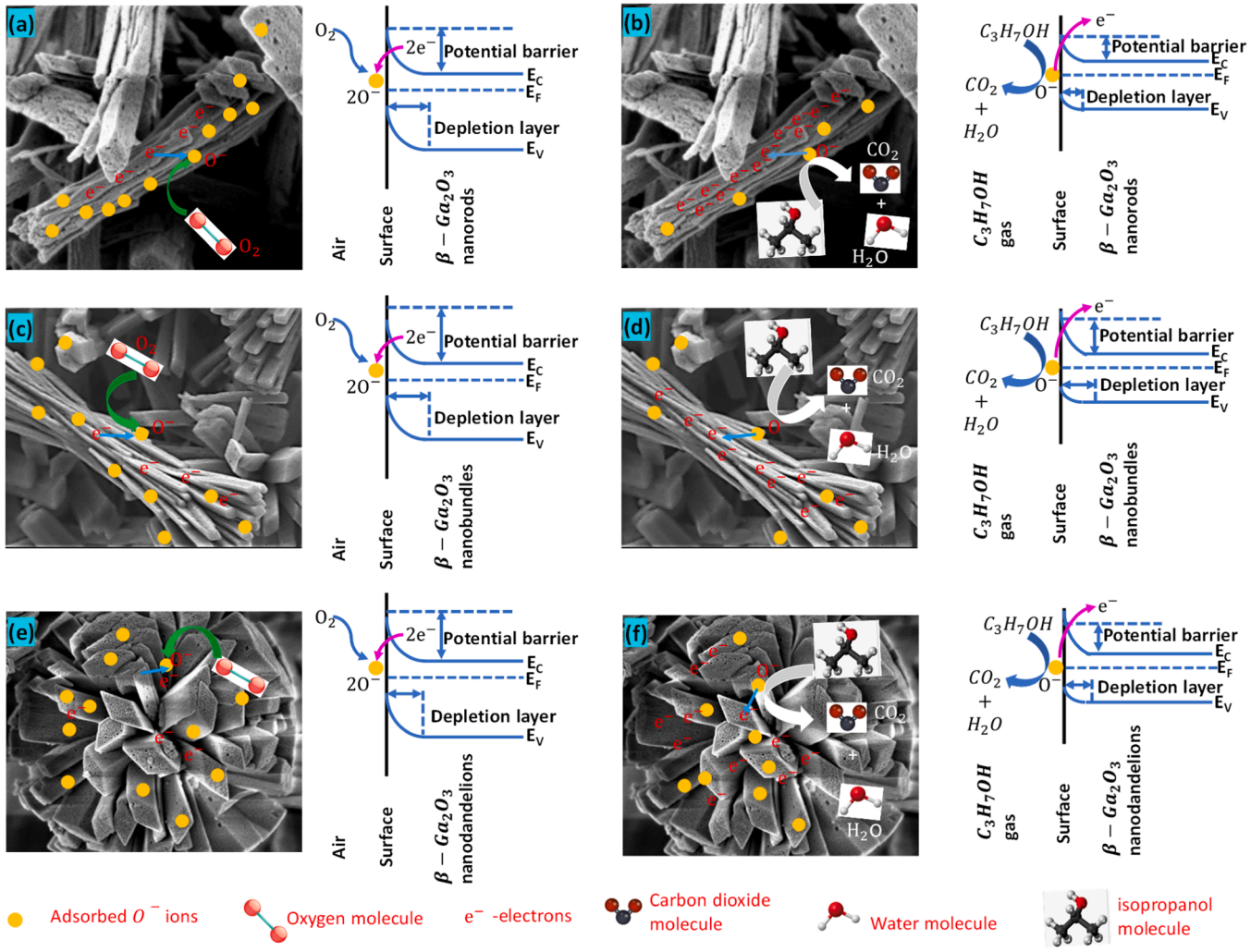

Fig. 7. Schematic representations and band diagrams of $\beta - Ga_2O_3$ (a, b) nanorods (pH7), (c, d) nanobundles (pH11) and (e, f) nanodandelions (pH14)-based gas sensors in air and towards isopropanol vapour.

charge transport channels. Furthermore, the nanobundles (pH11) and nanodandelions (pH14) presented the low limits of detection towards isopropanol, and this could be attributed to the preference of isopropanol molecules to attach to crevices sites present on the nanobundles and nanodandelions. This result indicated that the nanorod-based hierarchical morphological features may be ideal candidates for the detection of low concentrations of isopropanol.

4. Conclusion

In this study, we described the preparation of regular and hierarchical $\beta - Ga_2O_3$ nanorod-based nanostructures derived from the microwave-assisted hydrothermal method by variation of reaction pH conditions. Furthermore, structural, morphological, and compositional analysis of the nanostructures were conducted, and were correlated with the gas sensing performances of the nanostructures. The XRD results confirmed the synthesis of highly crystalline $\beta - Ga_2O_3$ powders while the FESEM micrographs revealed the crystallization of nanorods-like, nanobundles-like, and nanodandelion-like morphologies at pH levels of 7, 11 and 14, respectively with varying specific surface area and porosity demonstrated by the BET results. Furthermore, the XPS results revealed that the three different morphologies of $\beta - Ga_2O_3$ possessed different content of lattice oxygen, oxygen vacancies and chemisorbed oxygen species. Following the material characterization, gas sensing measurements were carried out and the results revealed that the $\beta - Ga_2O_3$ nanorods (pH7) presented high response towards isopropanol than the nanobundles (pH11) and nanodandelions (pH14). The highest response of 6.7 was recorded towards 90 *ppm* propanol from the $\beta - Ga_2O_3$ nanorods (pH7) at 150 °C. The high response from this morphology was explained in terms of the large specific surface area and the type of defects present on the surface of the sensing material. In addition, it was also observed that the nanobundles and nanodandelions morphologies of $\beta - Ga_2O_3$ presented fast response kinetics and high sensitivities, and this was attributed to the high contact networks in these morphologies which provide large number of charge transport channels. According to these results, it can be concluded controlling the nanorod-based morphology of $\beta - Ga_2O_3$ could provide methods of tuning the gas sensing performances (i.e. sensor response, response/recovery times and sensitivity) of this material which may be useful in the reliable real-time detection of isopropanol for indoor environments. All sensors presented lower resistance and longer response/recovery times in humid conditions. In addition, minor fluctuations were observed in the sensor stability over a one-month test period. However, further studies can be carried out to address these shortcomings. This can be through surface modification by noble metal nanoparticles or heterojunction formation with other metal oxides. Furthermore, incorporation of a hydrophobic materials during synthesis or sensor assembly in the form of a filter may reduce the access of the water vapour molecules to the sensing layers. As a result, the sensor response and response/recovery times are not greatly affected in humid conditions.

Declaration of competing interest

The authors declare that they have no known competing financial interests or personal relationships that could have appeared to influence the work reported in this paper.

Acknowledgments

The authors acknowledge funding from OWSD and Sida (Swedish International Development Cooperation Agency) - no. 3240315354, the National Research Foundation (NRF), South Africa and the Council for Scientific and Industrial Research (CSIR), South Africa (project no. C2F0099).

References

[1] X. Zhou, et al., Environmental and human health impacts of volatile organic compounds: a perspective review, Chemosphere 313 (2023) 137489.
[2] I. Manisalidis, et al., Environmental and health impacts of air pollution: a review, Front. Public Health 8 (2020) 14.
[3] World Health Organization, 2-Propanol, World Health Organization, 1990.
[4] H. Zhai, Z. Wu, Z. Fang, Recent progress of Ga_2O_3-based gas sensors, Ceram. Int. 48 (17) (2022) 24213–24233.
[5] T. Lin, et al., The morphologies of the semiconductor oxides and their gas-sensing properties, Sensors 17 (12) (2017) 2779.
[6] R. Pilliadugula, N.G. Krishnan, Effect of pH dependent morphology on room temperature NH_3 sensing performances of β-Ga_2O_3, Mater. Sci. Semicond. Process. 112 (2020) 105007.
[7] S. Park, et al., Synthesis, structure and ethanol sensing properties of Ga_2O_3-core/WO_3-shell nanostructures, Thin. Solid. Film. 591 (2015) 341–345.
[8] Y.-G. Jang, et al., Fabrication of Ga_2O_3/SnO_2 core–shell nanowires and their ethanol gas sensing properties, J. Mater. Res. 26 (17) (2011) 2322–2327.
[9] C. Jin, et al., Ultrasensitive multiple networked Ga_2O_3-core/ZnO-shell nanorod gas sensors, Sensor. Actuat. B: Chem. 161 (1) (2012) 223–228.
[10] J.I. Langford, A.J.C. Wilson, Scherrer after sixty years: a survey and some new results in the determination of crystallite size, J. Appl. Crystallogr. 11 (2) (1978) 102–113.
[11] G. Amin, et al., Influence of pH, precursor concentration, growth time, and temperature on the morphology of ZnO nanostructures grown by the hydrothermal method, J. Nanomater. 2011 (2011) 5. -5.
[12] A.C. Taş, P.J. Majewski, F. Aldinger, Synthesis of gallium oxide hydroxide crystals in aqueous solutions with or without urea and their calcination behavior, J. Am. Ceram. Soc. 85 (6) (2002) 1421–1429.
[13] D. Yue, et al., A facile synthesis and optical properties of bundle-shaped $TbPO_4{\cdot}H_2O$ nanorods, Adv. Condens. Matter Phys. 2013 (2013).
[14] T. Li, W. Zeng, New insight into the gas sensing performance of SnO_2 Nanorod-assembled urchins based on their assembly density, Ceram. Int. 43 (1) (2017) 728–735.
[15] M. Thommes, et al., Physisorption of gases, with special reference to the evaluation of surface area and pore size distribution (IUPAC Technical Report), Pure and Appl. Chem. 87 (9–10) (2015) 1051–1069.
[16] E. Ciftyurek, Z. Li, K. Schierbaum, Adsorbed oxygen ions and oxygen vacancies: their concentration and distribution in metal oxide chemical sensors and influencing role in sensitivity and sensing mechanisms, Sensors 23 (1) (2022) 29.
[17] N.C. Gatsi, et al., Hierarchically-ordered nanorods of Ga_2O_3 derived from microwave-assisted hydrothermal approach: investigation of calcination-induced structural evolution and optical behavior, Mater. Today Commun. 33 (2022) 104808.
[18] J.-C. Dupin, et al., Systematic XPS studies of metal oxides, hydroxides and peroxides, Phys. Chem. Chem. Phys. 2 (6) (2000) 1319–1324.
[19] C. Wang, et al., Metal oxide gas sensors: sensitivity and influencing factors, Sensors 10 (3) (2010) 2088–2106.
[20] V.E. Bochenkov, G.B. Sergeev, Sensitivity, selectivity, and stability of gas-sensitive metal-oxide nanostructures, Metal Oxide Nanostruct. Applic. 3 (2010) 31–52.
[21] M.I. Nemufulwi, H.C. Swart, G.H. Mhlongo, Enhanced propanol response behavior of $ZnFe_2O_4$ NP-based active sensing layer induced by film thickness optimization, Processes 10 (9) (2021) 1791.
[22] W.T. Honeycutt, M.T. Ley, N.F. Materer, Precision and limits of detection for selected commercially available, low-cost carbon dioxide and methane gas sensors, Sensors 19 (14) (2019) 3157.
[23] K. Dyndal, et al., CuO-Ga_2O_3 thin films as a gas-sensitive material for acetone detection, Sensors 20 (11) (2020) 3142.
[24] A. Afzal, β-Ga_2O_3 nanowires and thin films for metal oxide semiconductor gas sensors: sensing mechanisms and performance enhancement strategies, J. Materiom. 5 (4) (2019) 542–557.